

## Low-field AC susceptibility measurements on monocrystalline erbium

This article has been downloaded from IOPscience. Please scroll down to see the full text article.

1990 J. Phys.: Condens. Matter 2 3349

(<http://iopscience.iop.org/0953-8984/2/14/019>)

View [the table of contents for this issue](#), or go to the [journal homepage](#) for more

Download details:

IP Address: 171.66.16.103

The article was downloaded on 11/05/2010 at 05:51

Please note that [terms and conditions apply](#).

## Low-field AC susceptibility measurements on monocrySTALLINE erbium

H U Åström, D-X Chen, G Benediktsson and K V Rao

Department of Solid State Physics, Royal Institute of Technology, S-100 44 Stockholm, Sweden

Received 15 August 1989

**Abstract.** The magnetic properties of monocrySTALLINE erbium have been determined with low-field AC susceptibility measurements between 4.2 and 150 K for different frequencies and magnetic fields with the applied field parallel and perpendicular to the  $c$  axis. The real component of the susceptibility shows anomalies at the antiferromagnetic transition ( $T_N = 85$  K) and at the ferromagnetic transition ( $T_C = 19$  K) as well as for the basal plane ordering transition at 52 K and for commensurate transitions at 34 and 28 K. The magnetic effects at these transitions are discussed in relation to the results of previous calorimetric measurements on the same crystal. To account for the observed non-zero value of the imaginary part of the susceptibility at the transitions, different loss mechanisms are suggested.

### 1. Introduction

Erbium has a hexagonal close-packed lattice, with a complex but well known magnetic structure (see e.g., [1]). Erbium has a Néel temperature  $T_N$  of 85 K below which the  $c$  axis moments order in a sinusoidally modulated structure. Below about 52 K ( $T_H$ ) an additional component of the magnetic moment, ordered helicoidally in the basal plane, is developed while below 19 K ( $T_C$ ) a conical ferromagnetic structure with the net magnetic moment along the  $c$  axis appears. In most of the temperature range between  $T_C$  and  $T_H$ , the spin structure is incommensurate with the lattice. However, at certain temperatures, structures commensurate with the lattice over a certain number of atomic layers are developed. This occurs at 51 K (seven-atomic-layer period), 34 K (15-layer period), 27 K (23-layer period) and 25 K (eight-layer period) [2]. These structures are stable in a narrow temperature range. Between 25 K and  $T_C$  the magnetic structure remains commensurate with the lattice but for temperatures below about 22 K it attains a 'squared' configuration with half the components of the magnetic moment along the  $c$  axis parallel to and the other half antiparallel to this axis.

In a recent paper [3] we reported a calorimetric study of the magnetic transitions in monocrySTALLINE erbium. The ferromagnetic transition observed at 19.2 K gave an energy change of  $18.5 \pm 1.0$  J mol<sup>-1</sup>. With increasing temperature, small energy peaks of the order of 1 J mol<sup>-1</sup> were observed at 21.6, 23.3, 25.3, 50.8 and 53.4 K. The peak at 53.4 K is due to the basal plane ordering transition while the peaks at 25.3 and 50.8 K are probably caused by transitions to the commensurate structures with eight- and seven-layer periodicities, respectively. The peaks at 21.6 and 23.3 K (sometimes only one peak

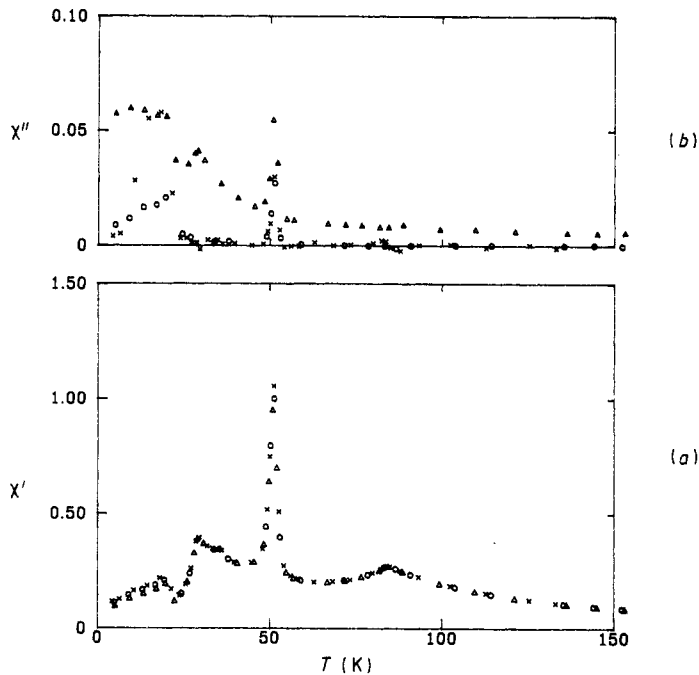


**Figure 1.** The AC susceptibility  $\chi'(T)$  and  $\chi''(T)$ , measured at an AC field amplitude of  $240 \text{ A m}^{-1}$ , applied parallel to the  $c$  axis for different frequencies:  $\times$ , 10 Hz;  $\circ$ , 100 Hz;  $\triangle$ , 1000 Hz. For clarity a reduced number of data points are shown in the figures.

at 21.6 K was obtained) may be connected with the 'squaring-up' transition or some kind of commensuration of the spin structure with the lattice. The Néel transition occurred at 85.6 K. The calorimetric measurements did not, however, detect the 23- or 15-layer commensurate transitions, which was surprising since the eight- and seven-layer structures were readily observed. Because of this inconsistency and in order to obtain a more direct correlation between the calorimetric data and the magnetic properties in erbium, we decided to undertake magnetic measurements on the same crystal which was used in the calorimetric study.

The magnetic properties of erbium have been the subject of several investigations. For magnetically strongly anisotropic materials such as erbium it is an advantage to use single crystals to avoid averaging the magnetic properties over different directions. Measurements of the DC susceptibility of monocrystalline erbium have been reported earlier [4, 5]. These studies were, however, undertaken only in the paramagnetic regime. Recently some reports on the magnetisation of pure erbium and erbium loaded with hydrogen have appeared [6–8]. Hydrogen was introduced into the lattice as a convenient way to change the electronic properties and hence the magnetic interactions.

For the present investigation we have chosen to study the AC susceptibility. From the real and imaginary (lossy) components of the AC susceptibility and their dependence on temperature  $T$ , frequency  $f$  and amplitude of the AC field  $H_m$ , complementary information about the magnetic transitions in relation to that of the DC susceptibility and magnetisation measurements can be obtained. The lossy component and its  $T$ -dependence shed light on the hysteretic effects, i.e. the nature of the domain structure

effects at the phase transitions. To the best of our knowledge there have been no AC susceptibility studies on monocrystalline erbium reported earlier.

## 2. Experimental details

The sample was obtained from a single crystal of erbium with a purity of 99.9 at.% or better kindly put at our disposal by D Fort, Department of Metallurgy and Materials, University of Birmingham. From this crystal, samples for both the calorimetric and the susceptibility measurements were cut. The sample for the susceptibility studies was a rectangular parallelepiped of dimensions 2.9 mm  $\times$  3.0 mm  $\times$  1.9 mm with the  $c$  axis approximately, to within a few degrees, parallel to the shortest edge of the sample.

The AC susceptometer used was an unbalanced mutual impedance bridge with a concentric coil system, calibrated by cylindrical samples of lead and copper. For each run the sample was under fixed AC field and the frequency was periodically changed between 10, 100 and 1000 Hz. The applied AC fields were 240 A m<sup>-1</sup> (3 Oe) and 8000 A m<sup>-1</sup> (100 Oe), the latter being the highest field attainable with the present equipment. The AC susceptibility was measured with the field either along the  $c$  axis or in the basal plane with a direction close to the  $a$  (easy) axis. To obtain the final results of the susceptibility, appropriate demagnetisation corrections were made. The susceptibility was measured from 4.2 to 150 K at a warming rate of 0.5–2 K min<sup>-1</sup>. The data were always taken during warming in order to avoid thermal hysteresis effects.

## 3. Results

### 3.1. AC field parallel to the $c$ axis

Figure 1(a) reports the real component  $\chi'$  of the susceptibility as a function of  $T$  for  $f = 10$  Hz (crosses), 100 Hz (open circles) and 1000 Hz (open triangles) with the field  $H_m = 240$  A m<sup>-1</sup> applied parallel to the  $c$  axis. On the curves, five maxima or break points in the temperature dependence of  $\chi'$  are visible at 19, 28, 34, 52 and 85 K. In figure 2(a),  $\chi'$  for the higher field (8000 A m<sup>-1</sup>) is shown for  $f = 10$  Hz (full circles). For comparison the curve for  $H_m = 240$  A m<sup>-1</sup> and 10 Hz is replotted in the figure (broken curve). It is obvious that increasing the field by a factor of 33 does not change  $\chi'$  much except that at 52 K and below 20 K there is a significant enhancement of  $\chi'$  for the higher field. The frequency dependence of  $\chi'$  is very small in most of the temperature range studied except at 52 K and at the lowest temperatures where there is a small decrease in  $\chi'$  with increasing frequency.

For the imaginary component  $\chi''$  of the susceptibility the curves look more complicated. At the lower field (figure 1(b)),  $\chi''$  increases with decreasing temperature for a fixed frequency. This behaviour is typical for an eddy current effect and is due to the decrease in the resistivity with decreasing temperature. It is also evident that  $\chi''$  increases with increasing frequency. This is also a result which is predicted by the classical eddy current theory. For all three frequencies a narrow peak appears in  $\chi''$  at 52 K while at 28 K a small maximum is obtained only for the highest frequency. Below 20 K a strong enhancement of  $\chi''$  is observed for 10 Hz. Increasing the field to 8000 A m<sup>-1</sup> (figure 2(b)) leads to a further strengthening of this peak.

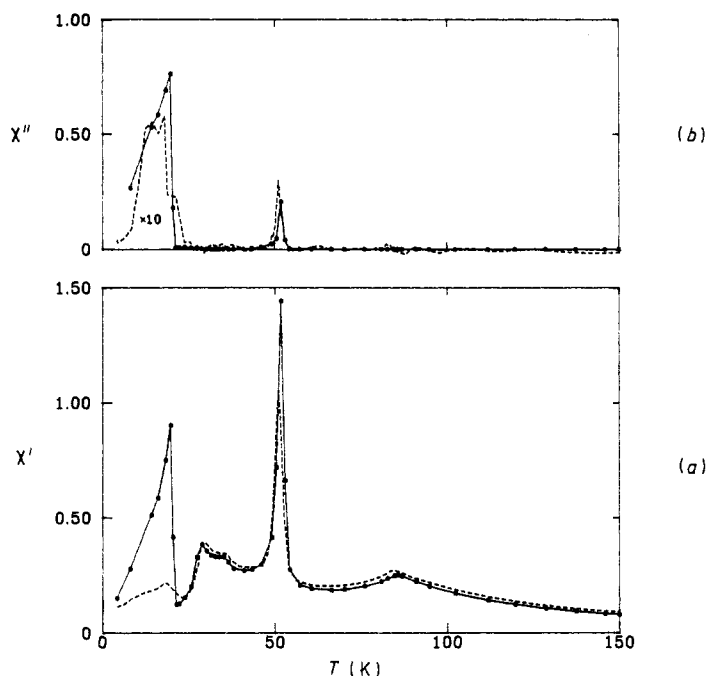


**Figure 2.** The AC susceptibility versus temperature at 10 Hz with the field  $8000 \text{ A m}^{-1}$  parallel to the  $c$  axis (●): —, guides for the eye. For comparison the corresponding data for  $H_m = 240 \text{ A m}^{-1}$  have been plotted (- - -). Note that  $\chi''(T)$  for  $240 \text{ A m}^{-1}$  is plotted on a scale  $\times 10$ .

### 3.2. AC field along the basal plane

In figure 3(a),  $\chi'$  is plotted versus  $T$  for  $f = 10 \text{ Hz}$  (crosses),  $100 \text{ Hz}$  (open circles) and  $1000 \text{ Hz}$  (open triangles) with the field ( $240 \text{ A m}^{-1}$ ) along the basal plane. The maxima at 28 and 52 K can still be observed but instead of a peak at 19 K a sharp drop occurs. The shoulder at 34 K and the peak at 85 K are only visible as weak changes in the slope of the curves. There is no significant frequency dependence to be seen from the results in figure 3(a). Increasing the field to  $8000 \text{ A m}^{-1}$  leads only to a small overall decrease in  $\chi'$ . For the  $\chi''$  component (figure 1(b)) the trend of the temperature and frequency dependences from figure 1(b) is maintained. The peaks at 28 and 52 K are virtually missing but below 20 K a small maximum is observed for the lowest frequency. The higher field,  $8000 \text{ A m}^{-1}$ , has no greater influence on  $\chi''$ . Figure 4 shows a comparison between  $\chi$  for the  $c$  axis (full circles) and basal plane (broken curve) orientations for  $H_m = 8000 \text{ A m}^{-1}$  and  $f = 10 \text{ Hz}$ . The inset is an enlargement of the region around  $T_N$ .

The magnetic moment in the paramagnetic range was calculated from a Curie–Weiss fit of the  $\chi'$  data between 110 and 150 K for the  $c$  axis and basal plane orientations of the magnetic field. The value of the moment obtained was  $(9.7 \pm 0.2)\mu_B$ . The corresponding paramagnetic Curie temperatures were determined to  $60 \pm 1$  and  $38 \pm 2 \text{ K}$  for the  $c$  axis and basal plane orientations of the field.

## 4. Discussion

With increasing temperature the maxima and anomalies appearing on the  $\chi'$  curves correspond to the ferromagnetic transition (19 K), the 23-layer commensurate (28 K),

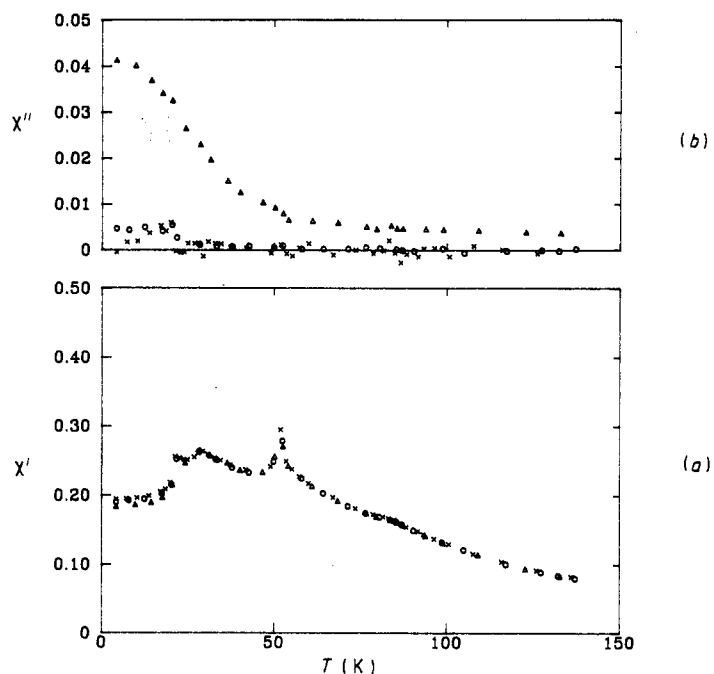


Figure 3. The AC susceptibility  $\chi'(T)$  and  $\chi''(T)$  with a field of  $240 \text{ A m}^{-1}$  in the basal plane for different frequencies:  $\times$ , 10 Hz;  $\circ$ , 100 Hz;  $\triangle$ , 1000 Hz.

the 15-layer commensurate (34 K), the incommensurate helicoidal basal plane ordering (52 K) and the antiferromagnetic  $c$  axis modulated to paramagnetic (85 K) transitions, respectively, as identified by comparison with the temperature dependence of the wavevector of erbium [2]. In the following, these transitions and their loss mechanisms will be discussed on the basis of the AC susceptibility results.

#### 4.1. The ferromagnetic transition

In the ferromagnetic state there should be a domain structure in the crystal with the magnetisation in most of the domains parallel or antiparallel to the  $c$  axis. When the applied field along the  $c$  axis is small ( $240 \text{ A m}^{-1}$ ), the magnetisation process is due to reversible domain wall displacements. At the higher field ( $8000 \text{ A m}^{-1}$ ), some irreversible wall displacements take place, explaining the increase in  $\chi'$ . In contrast to the maximum in  $\chi'$ , when the field is along the  $c$  axis a drop in the susceptibility occurs for the perpendicular orientation of the field (figure 3(a)). A similar result can be found in the magnetisation curves of Burger *et al* [8]. The decrease in  $\chi'$  for the basal plane orientation could be explained by the fact that the  $c$  axis component of the magnetic moment for  $T < T_C$  is smaller than that for  $T > T_C$  [1]. As the susceptibility with the field in the basal plane is determined by the average torque experienced by the  $c$  axis moments,  $\chi'$  should in this case decrease at  $T_C$  with decreasing temperature.

#### 4.2. The magnetic transitions between $T_C$ and $T_H$

In the temperature range between  $T_C$  and  $T_H$ , several commensurate transitions occur. The anomalies in  $\chi'$  observed at 28 and 34 K can be identified with transitions to

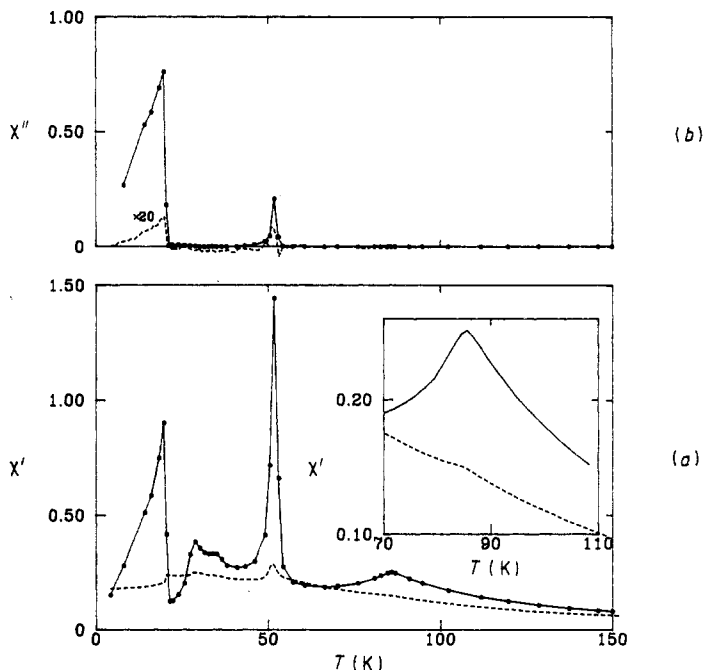


Figure 4.  $\chi'(T)$  and  $\chi''(T)$  at 10 Hz with a field of  $8000 \text{ A m}^{-1}$  parallel to the  $c$  axis (●) or in the basal plane (---): —, guides for the eye. Note that  $\chi''(T)$  for the basal plane is plotted on a scale  $\times 20$ . The inset shows an enlargement of the region around the Néel point.

commensurate structures of 23- and 15-layer periodicity. These commensurate structures have a small net magnetic moment along the  $c$  axis [2] which will explain the anomalies in the  $c$  axis  $\chi'$  at these temperatures. The basal plane susceptibility should not be affected unless there is a coupling between the  $c$  axis and basal plane components of the moment. In fact, small changes in  $\chi'$  with the field along the basal plane can be detected which speaks in favour of the existence of some coupling in this case. These commensurate transitions were not observed in the calorimetric measurements [3]. Probably the changes in magnetoelastic energy which are responsible for the main part of the energy changes at the magnetic transitions at these temperatures are too small to be detected in the calorimetric measurements. On the other hand an energy change of about  $1 \text{ J mol}^{-1}$  was observed at 25.3 K. We believe that this energy change is due to the commensurate transition with an eight-layer periodicity which was observed in [2]. This structure does not possess a net magnetic moment along the  $c$  axis as the period extends over an even number of atomic layers and should therefore not lead to an enhancement of the susceptibility measured with the field in the  $c$  direction. This is in accord with the results for  $\chi'$  which in fact show extremely low values, lower than that of  $\chi'$  for the basal plane, for temperatures between 25 K and  $T_C$ . Anomalously low values of the magnetisation in this temperature range is also present in earlier investigations [6, 7]. The 'squaring-up' of the  $c$  axis moments may also contribute to the low value of  $\chi'$ . In a field applied parallel to the basal plane the torque on the moments will become larger as a result of the 'squaring-up', while the torque in a field along the  $c$  direction will decrease, leading to a lower susceptibility in this case.

The transition at 51 K to a commensurate structure with a seven-layer periodicity, which carries a magnetic moment as the period extends over an odd number of atomic

layers, is not detectable in  $\chi'$ , nor was it observed in the earlier magnetisation results [6, 7]. This transition is, however, so close in temperature to the basal plane ordering transition that it may be masked by the dramatic increase in  $\chi'$  at the later transition.

The sharp increase in  $\chi'$  at 52 K (figure 1(a)) shows a ferromagnetic-like divergence. It is also highly anisotropic with only a small peak in  $\chi'$  for the basal plane (figure 3(a)). It is obvious that the occurrence of ordering of the moments in the basal plane strongly modifies the magnetisation in the perpendicular direction. It is well known that there is a significant onset of lattice expansion along the  $c$  axis with decreasing temperature concomitant with a gradual contraction along the basal plane to minimise the magnetoelastic energy. Such redistribution of strains modifies the domain configuration and the conduction electrons as well via the 4f ions during the lattice distortion. Furthermore the magnetic ordering will introduce superzone boundaries with gaps at the Fermi surface. These gaps will change the energy of the electrons as well as the effective exchange interaction between the localised magnetic moments and hence influence both the electrical and the magnetic properties along certain crystallographic directions. This can be expected to be particularly pronounced for the magnetic transition at  $T_H$  in erbium with its two different types of antiferromagnetic ordering. Superzone effects modify in this case the shape of the resistivity curve so that the  $c$  axis resistivity shows a sharp break point at  $T_H$  while only weak changes appear in the basal plane resistivity [9]. This is to be compared with the situation for the susceptibility which changes strongly in the  $c$  axis direction but only slightly when the field is along the basal plane. Superzone effects will certainly play an important role also for the susceptibility changes at this transition.

#### 4.3. The antiferromagnetic transition

While a peak is observed at  $T_N$  in  $\chi'$  with the field parallel to the  $c$  axis, the effect of the antiferromagnetic transition on the basal plane susceptibility is observable only as a weak change in the slope of the  $\chi'$  curve (see inset to figure 4(a)). This anisotropic behaviour is typical for antiferromagnetic transitions in magnetically uniaxial materials. In this case, if the ordering takes place along the  $c$  axis, the susceptibility in this direction will show a peak at  $T_N$  while the susceptibility with the field in the basal plane should be virtually constant immediately below  $T_N$ .

The magnetic moment in the paramagnetic range obtained from our susceptibility data ( $9.7 \pm 0.2$ ) $\mu_B$ , is in accord with the theoretical value,  $9.6\mu_B$ , and a reported [4] experimental determination of  $(9.9 \pm 0.2)\mu_B$ . The paramagnetic Curie temperatures,  $60 \pm 1$  and  $38 \pm 2$  K, for the  $c$  axis and the basal plane orientations, are also consistent with the reported values [4] of 61.7 and 32.5 K.

#### 4.4. Loss mechanisms

The non-zero value of  $\chi''$  comes from different kinds of losses during the AC magnetisation process. Moreover, lattice distortion and the consequent changes in the exchange energy at the intermediate spin transitions in erbium are rather large and anisotropic. This results in a domain configuration which readjusts itself to minimise the magnetoelastic energy at these transitions and manifests a non-zero  $\chi''$ , especially along the  $c$  axis.



An obvious loss mechanism is due to eddy currents. For a paramagnetic magnetisation process the classical eddy current loss theory [10] can be applied. In this case, for a cylinder of radius  $a$ ,  $\chi'$  and  $\chi''$  determined by eddy currents are

$$\chi' = \chi_0 - (1 + \chi_0)\theta^4/48 \quad (1)$$

and

$$\chi'' = (1 + \chi_0)\theta^2/8 \quad (2)$$

where  $\chi_0$  is the DC susceptibility and  $\theta$  is a function of  $a$  and the skin depth  $s$ :

$$\theta = a\sqrt{2}/s \quad (3)$$

$s$  is determined by the resistivity  $\rho$ ,  $\chi_0$  and the frequency  $f$ :

$$s = 5.03 \times 10^2 \sqrt{\rho/(1 + \chi_0)f}. \quad (4)$$

Equations (1) and (2) are derived for  $\theta \ll 1$ , a condition which is satisfied in the present case.

A simple check of the validity of the classical eddy current model is to calculate  $\chi'$  and  $\chi''$  at 100 K with the field along the  $c$  axis. Assuming a value of  $0.56 \mu\Omega \text{ m}$  for the resistivity along the basal plane [4], a value of  $1.7 \times 10^{-3} \text{ m}$  for the average sample radius, and an approximate value of 0.20 for  $\chi_0$  from figure 1, equations (1)–(4) give  $\chi' = 0.0074$  for 1000 Hz, which is consistent with our observed experimental value of 0.0077. The decrease in  $\chi'$  relative to the DC susceptibility is  $-0.6 \times 10^{-4}$ , also consistent with the invisible frequency dependence in the experimental results in figure 1. From similar calculations for the spin configurations at 52 K, 28 K and 4.2 K, one obtains  $\chi'' = 0.031$ , 0.021 and 0.019 respectively. These values are, however, larger by a factor of 2–3 than those observed experimentally (figure 1(b)). The decrease in  $\chi'$  with increasing frequency in figure 1(a) is also much larger than the calculated values. Similar results are found for the data at the higher field and for the susceptibility with the field along the basal plane. Hence the classical eddy current mechanism cannot alone explain quantitatively the observed susceptibility behaviour.

The classical eddy current theory assumes a constant scalar susceptibility. In highly anisotropic magnetically ordered materials such as erbium a tensor susceptibility has to be introduced. Furthermore, because of the complex domain structure which readjusts itself at each of the intermediate spin configurations, lateral eddy current losses around the domain structure should be taken into account. Such additional contributions will, however, only be second-order effects and cannot account for the observed large changes in  $\chi''(T)$  at the 52 K transition. This suggests that contributions to  $\chi''$  from relaxation effects may also have to be taken into account at the magnetic transitions in erbium. The marked peak in  $\chi''$  below 20 K for 10 Hz (figure 1(b)) could be considered to indicate this. The relaxation time is in this case of the order of 0.1 s, which is of the same magnitude as the time scale for domain wall displacements.

## 5. Conclusions

The low-field AC susceptibility measured along the  $c$  axis shows maxima or other anomalies at 19 K, 28 K, 34 K, 52 K and 85 K corresponding to the ferromagnetic, the 23-layer commensurate, the 15-layer commensurate, the incommensurate helicoidal basal plane ordering and the antiferromagnetic  $c$  axis modulated to paramagnetic transitions,

respectively. The transition to the eight-layer commensurate structure at 25 K, observed calorimetrically on the same crystal, did not give rise to any maximum in the susceptibility. On the contrary the  $c$  axis susceptibility has an anomalously low value between 25 K and  $T_C$  (19 K) compared with the basal plane susceptibility. The reason for this might be that the eight-layer commensurate structure does not carry a net magnetic moment in contrast to the other commensurate structures, thus leading to a lower susceptibility.

The  $c$  axis susceptibility shows a strong peak at the basal plane ordering transition at 52 K which is highly anisotropic with only a small peak in the basal plane susceptibility. The occurrence of spin ordering in the basal plane seems to have a strong influence on the magnetisation in the perpendicular direction. It is suggested that superzone gap effects which have a strong influence on the changes in the resistivity at  $T_H$  may also be important for the anisotropic susceptibility behaviour at this transition.

To account for the non-zero value of the imaginary part of the AC susceptibility, possible contributions from loss mechanisms are discussed. It is concluded that normal eddy current effects cannot alone explain the losses observed at the magnetic transitions, but there will probably also be contributions to  $\chi(T)$  at the transitions from relaxation effects. For a quantitative understanding of the losses due to changes in the spin configurations at the magnetic transitions, detailed consideration of the changes in the magnetoelastic energy and their concomitant effects on the conduction electrons via the 4f ions is, however, needed.

### Acknowledgments

We are indebted to J Nogues for valuable assistance in the preparation of the graphs. The work has been supported by the Swedish Natural Research Council and the Swedish Board for Technical Development (STU).

### References

- [1] Coqblin B 1977 *The Electronic Structure of Rare Earth Metals and Alloys* (London: Academic) p 52
- [2] Gibbs D, Bohr J, Axe J D, Moncton D E and D'Amigo K L 1986 *Phys. Rev. B* **34** 8182
- [3] Åström H U and Benediktsson G 1989 *J. Phys.: Condens. Matter* **1** 4381
- [4] Green R W, Legvold S and Spedding F H 1961 *Phys. Rev.* **122** 827
- [5] Aleonard R, Boutron P and Bloch D 1969 *J. Phys. Chem. Solids* **30** 2277
- [6] Ito T, Legvold S and Beaudry B J 1984 *Phys. Rev. B* **30** 240
- [7] Burger J P, Vajda P, Daou J N and Chouteau G 1986 *J. Phys. F: Met. Phys.* **16** 1275
- [8] Burger J P, Vajda P, Daou J N and Chouteau G 1987 *J. Magn. Magn. Mater.* **67** 343
- [9] Elliot R J and Wedgwood F A 1963 *Proc. Phys. Soc.* **81** 846; 1964 *Proc. Phys. Soc.* **84** 63
- [10] Bozorth R M 1951 *Ferromagnetism* (London: Van Nostrand) p 769